High-Temperature Non-Equilibrium CO_2 Kinetic and Radiation Processes

João Vargas

13th November 2020, PhD Defense

INSTITUTO DE PLASMAS
E FUSÃO NUCLEAR

Motivation - Mars

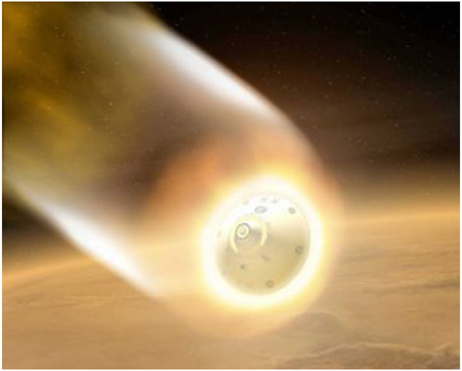

Image credit: JPL, jpl.nasa.gov

- Exploration: 6 missions launched in 2020, 3 to land in 2021

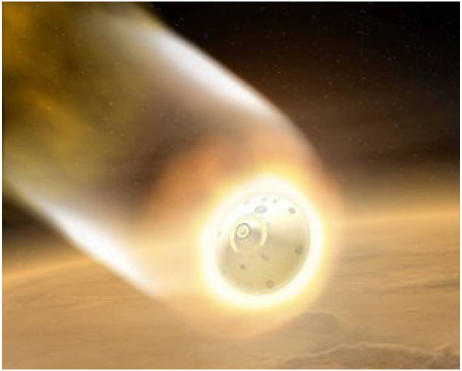

Image credit: JPL, jpl.nasa.gov

- Exploration: 6 missions launched in 2020, 3 to land in 2021
- Mars is a challenging planet to land: Thin atmosphere, mostly composed of CO_2

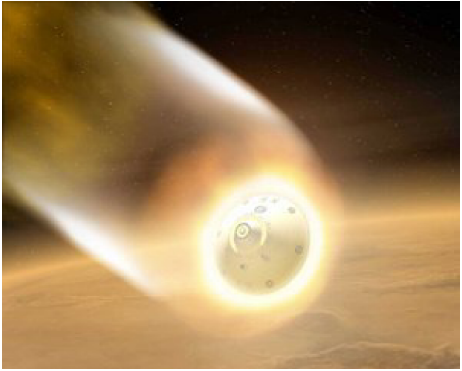

Image credit: JPL, jpl.nasa.gov

- Exploration: 6 missions launched in 2020, 3 to land in 2021
- Mars is a challenging planet to land: Thin atmosphere, mostly composed of CO_2
- Need to account for convective and radiative heating

Heatshield design

Relevance of CO_2 IR radiative heating only recognized in recent years

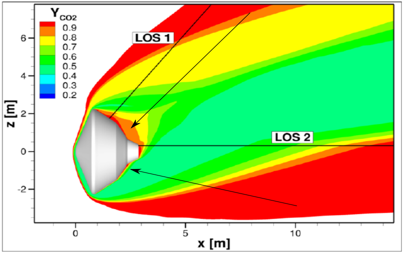

Image credit: Sahai, 2019

Heatshield design

Relevance of CO_2 IR radiative heating only recognized in recent years

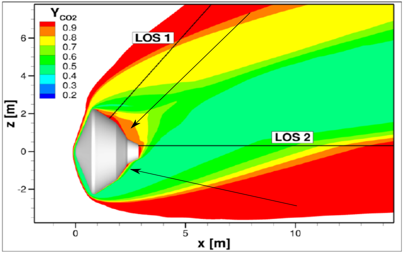

Image credit: Sahai, 2019

Radiation and kinetics are tightly coupled in atmospheric entry flows

Heatshield design

Relevance of CO_2 IR radiative heating only recognized in recent years

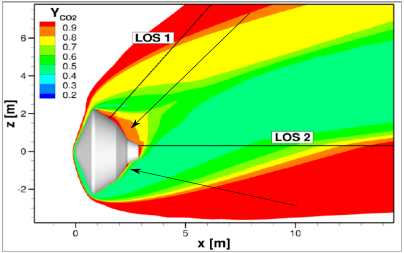

Image credit: Sahai, 2019

Radiation and kinetics are tightly coupled in atmospheric entry flows

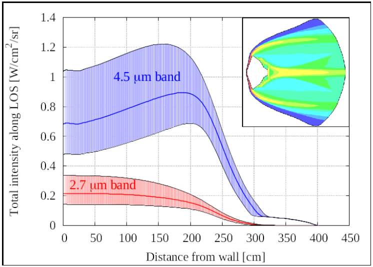

Image credit: Sahai, 2019

Detailed models are required which can be translated to engineering design tools

State-to-State Models

State-to-State models potentially provide the greatest levels of detail

Macroscopic:

- Assumed internal distribution characterized by a temperature

State-to-State Models

State-to-State models potentially provide the greatest levels of detail

Macroscopic:

- Assumed internal distribution characterized by a temperature

State-to-State

- Internal states are treated individually

State-to-State Models

State-to-State models potentially provide the greatest levels of detail

Macroscopic:

- Assumed internal distribution characterized by a temperature

State-to-State

- Internal states are treated individually

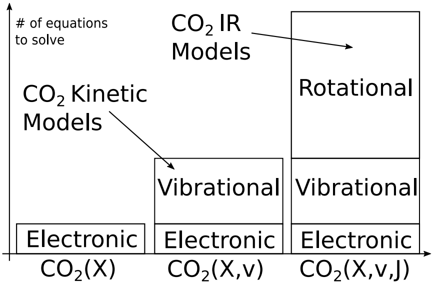

State-to-State Models

State-to-State models potentially provide the greatest levels of detail

Macroscopic:

- Assumed internal distribution characterized by a temperature

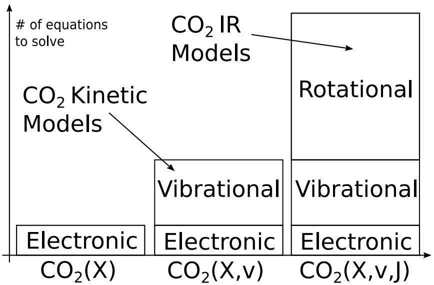

State-to-State

- Internal states are treated individually

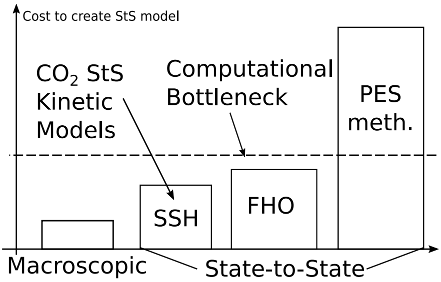

Shortcomings of CO_2 models

State of the art state-to-state (StS) kinetic models of CO_2 are based on SSH:

Shortcomings of CO_2 models

State of the art state-to-state (StS) kinetic models of CO_2 are based on SSH:

- Extrapolate badly

Shortcomings of CO_2 models

State of the art state-to-state (StS) kinetic models of CO_2 are based on SSH:

- Extrapolate badly
- Do not allow multi-quantum jumps

Shortcomings of CO_2 models

State of the art state-to-state (StS) kinetic models of CO_2 are based on SSH:

- Extrapolate badly
- Do not allow multi-quantum jumps
- Dissociation is not handled in the most correct way

Shortcomings of CO_2 models

State of the art state-to-state (StS) kinetic models of CO_2 are based on SSH:

- Extrapolate badly
- Do not allow multi-quantum jumps
- Dissociation is not handled in the most correct way
- Questions regarding coupling of symmetric and bending mode

Recent works rely on SSH models, there is room for improvement.

Shortcomings of CO_2 models

State of the art state-to-state (StS) kinetic models of CO_2 are based on SSH:

- Extrapolate badly
- Do not allow multi-quantum jumps
- Dissociation is not handled in the most correct way
- Questions regarding coupling of symmetric and bending mode

Recent works rely on SSH models, there is room for improvement.

The gold standard for high-T CO_2 IR radiation, CDSD4000:

Shortcomings of CO_2 models

State of the art state-to-state (StS) kinetic models of CO_2 are based on SSH:

- Extrapolate badly
- Do not allow multi-quantum jumps
- Dissociation is not handled in the most correct way
- Questions regarding coupling of symmetric and bending mode

Recent works rely on SSH models, there is room for improvement.

The gold standard for high-T CO_2 IR radiation, CDSD4000:

- Large database

Shortcomings of CO_2 models

State of the art state-to-state (StS) kinetic models of CO_2 are based on SSH:

- Extrapolate badly
- Do not allow multi-quantum jumps
- Dissociation is not handled in the most correct way
- Questions regarding coupling of symmetric and bending mode

Recent works rely on SSH models, there is room for improvement.

The gold standard for high-T CO_2 IR radiation, CDSD4000:

- Large database
- Computationally prohibitive for full spectrum calculations

Shortcomings of CO_2 models

State of the art state-to-state (StS) kinetic models of CO_2 are based on SSH:

- Extrapolate badly
- Do not allow multi-quantum jumps
- Dissociation is not handled in the most correct way
- Questions regarding coupling of symmetric and bending mode

Recent works rely on SSH models, there is room for improvement.

The gold standard for high-T CO_2 IR radiation, CDSD4000:

- Large database
- Computationally prohibitive for full spectrum calculations
- Cannot separate between vib. and rot. modes

A smaller, more compact database is desirable.

Shortcomings of CO_2 models

State of the art state-to-state (StS) kinetic models of CO_2 are based on SSH:

- Extrapolate badly
- Do not allow multi-quantum jumps
- Dissociation is not handled in the most correct way
- Questions regarding coupling of symmetric and bending mode

Recent works rely on SSH models, there is room for improvement.

The gold standard for high-T CO_2 IR radiation, CDSD4000:

- Large database
- Computationally prohibitive for full spectrum calculations
- Cannot separate between vib. and rot. modes

A smaller, more compact database is desirable.

This presentation will showcase new models that curtail these shortcomings

Outline

Kinetics

CO_2 Kinetic Modelling - Assumptions

Symmetric - v_1

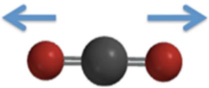

Bending - $v_2^{l_2}$

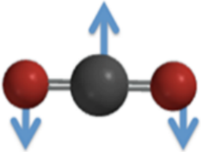

Asymmetric - v_3

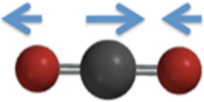

CO_2 Kinetic Modelling - Assumptions

Symmetric - v_1

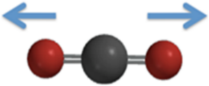

Bending - $v_2^{l_2}$

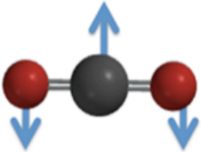

Asymmetric - v_3

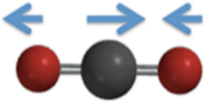

Mode separability

CO_2 Kinetic Modelling - Assumptions

Symmetric - v_1 Bending - $v_2^{l_2}$ Asymmetric - v_3

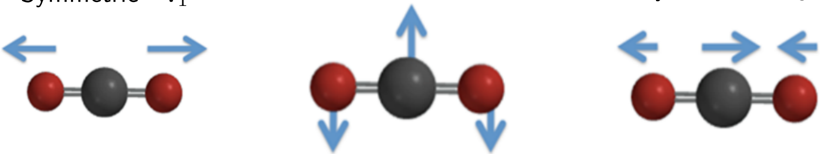

Mode separability

No Potential Energy Surface (PES) of CO_2 accurate up to dissociation. Each mode breaks apart in different ways.

- v_1: CO_2 + 18.53 eV $\rightarrow$ C + O + O
- v_2: CO_2 + 11.45 eV $\rightarrow$ C + O_2
- v_3: CO_2 + 7.42 eV $\rightarrow$ CO + O

Limits allows potential reconstruction by extrapolation of NASA-Ames-2 PES

CO_2 Kinetic Modelling - Assumptions

Symmetric - v_1 | Bending - $v_2^{l_2}$ | Asymmetric - v_3

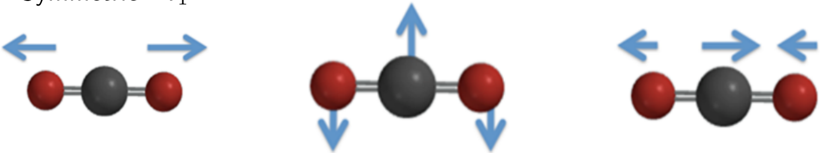

Mode separability

No Potential Energy Surface (PES) of CO_2 accurate up to dissociation. Each mode breaks apart in different ways.

- v_1: CO_2 + 18.53 eV $\rightarrow$ C + O + O
- v_2: CO_2 + 11.45 eV $\rightarrow$ C + O_2
- v_3: CO_2 + 7.42 eV $\rightarrow$ CO + O

Limits allows potential reconstruction by extrapolation of NASA-Ames-2 PES

Consider only extreme states

$$\text{Extreme states} = \begin{cases} v_1 0^0 0 \\ 0 v_2^{l_2} 0 \\ 0 0^0 v_3 \end{cases}$$

$$\text{Mixed states} = v_1 v_2^{l_2} v_3$$

Also limit $v_2 = l_2$, otherwise computationally untenable

Forced Harmonic Oscillator

The Forced Harmonic Oscillator (FHO) - 1D collision geometry, generalized to 3D with steric factors

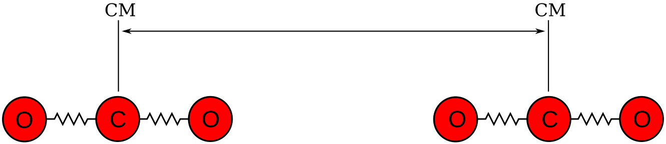

Forced Harmonic Oscillator

The Forced Harmonic Oscillator (FHO) - 1D collision geometry, generalized to 3D with steric factors

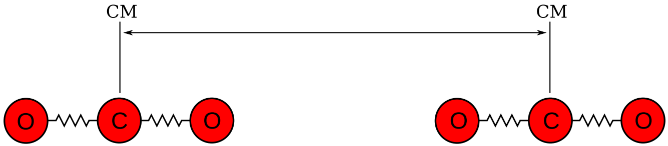

- Physically consistent extrapolation

Forced Harmonic Oscillator

The Forced Harmonic Oscillator (FHO) - 1D collision geometry, generalized to 3D with steric factors

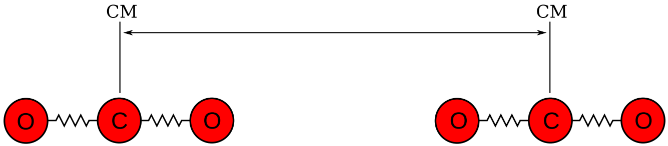

- Physically consistent extrapolation
- Handles multi quantum jumps

Forced Harmonic Oscillator

The Forced Harmonic Oscillator (FHO) - 1D collision geometry, generalized to 3D with steric factors

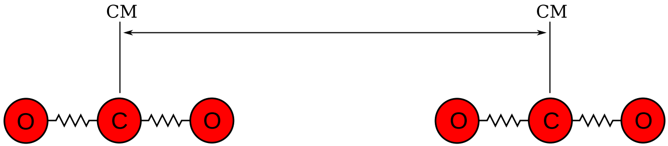

- Physically consistent extrapolation
- Handles multi quantum jumps
- $CO_2(X)$ and $CO_2(B)$ modeled through FHO

Ground State Level Manifold

- Low lying levels are obtained through Chédin (1984) polynomial expansion
- Sym. and Asym. stretch high lying levels are obtained through Schrödinger's equation
- Bending levels can be "safely" extrapolated, Quapp (1993)

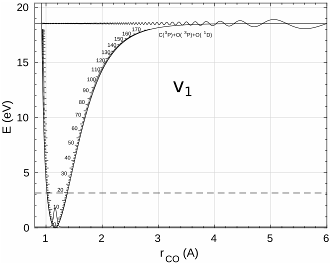

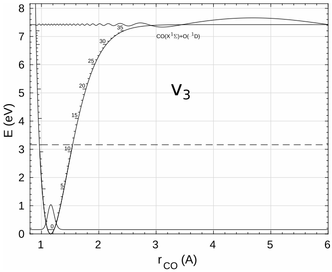

Ground State Level Manifold

- Low lying levels are obtained through Chédin (1984) polynomial expansion
- Sym. and Asym. stretch high lying levels are obtained through Schrödinger's equation
- Bending levels can be "safely" extrapolated, Quapp (1993)

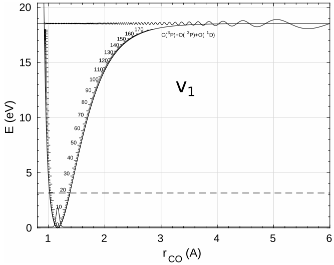

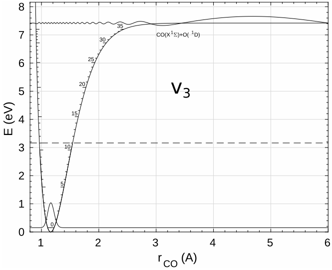

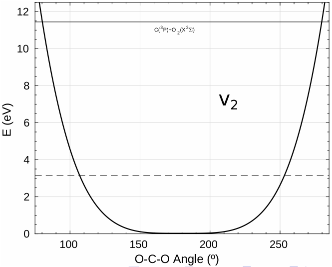

$^3B_2$ Level Manifold

In Grebenshchikov (2017) some vib. levels of $CO_2(^3B_2)$ are tabulated. These are used to obtain the coefficients of the polynomial expression:

$$E(v_1, v_2, v_3) = \sum_{i=1,2,3} \omega_i v_i + \sum_{i=1,2,3} x_{ii} v_i^2 + x_{12} v_1 v_2 + x_{13} v_1 v_3 + x_{23} v_2 v_3$$

$^3B_2$ Level Manifold

In Grebenshchikov (2017) some vib. levels of $CO_2(^3B_2)$ are tabulated. These are used to obtain the coefficients of the polynomial expression:

$$E(v_1, v_2, v_3) = \sum_{i=1,2,3} \omega_i v_i + \sum_{i=1,2,3} x_{ii} v_i^2 + x_{12} v_1 v_2 + x_{13} v_1 v_3 + x_{23} v_2 v_3$$

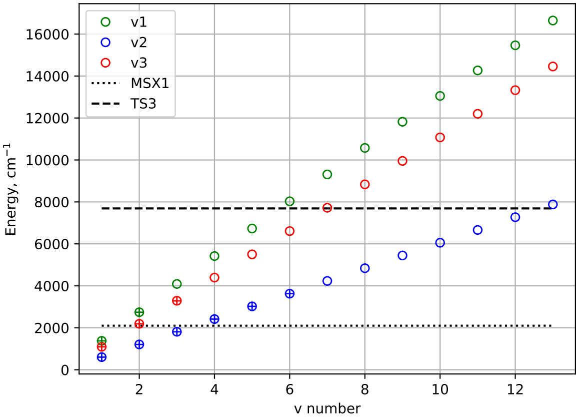

MSX1 - Crossing energy between ground and $^3B_2$

TS3 - Dissociation energy of $^3B_2$

VT and VVT

Including the first reactions

- Obtain semi-empirical parameters to fit FHO to known rates
- Extrapolate to the whole level manifold
- No rates for CO_2(B), use the same parameters as CO_2(X)

VT and VVT

Including the first reactions

- Obtain semi-empirical parameters to fit FHO to known rates
- Extrapolate to the whole level manifold
- No rates for $CO_2(B)$, use the same parameters as $CO_2(X)$

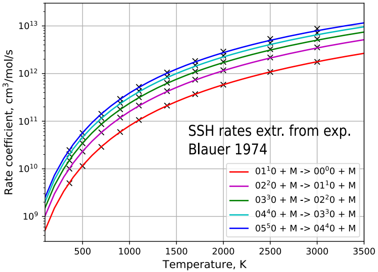

Vibration-Translation

$$CO_2(X,v') + M \longleftrightarrow CO_2(X,v'') + M$$

v' and v'' belong to the same vib. mode.

VT and VVT

Including the first reactions

- Obtain semi-empirical parameters to fit FHO to known rates
- Extrapolate to the whole level manifold
- No rates for $CO_2(B)$, use the same parameters as $CO_2(X)$

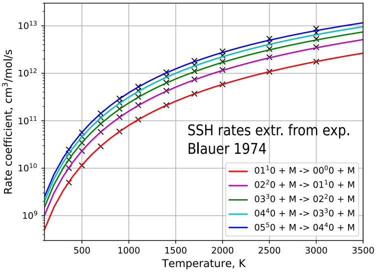

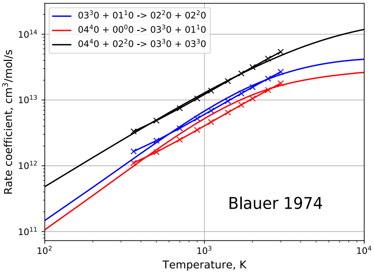

Vibration-Translation

$CO_2(X,v') + M \longleftrightarrow CO_2(X,v'') + M$

v' and v'' belong to the same vib. mode.

Vibration-Vibration-Translation

$CO_2(X,v) + CO_2(X,v) \longleftrightarrow CO_2(X,v+1) + CO_2(X,v-1)$

Model Schematic

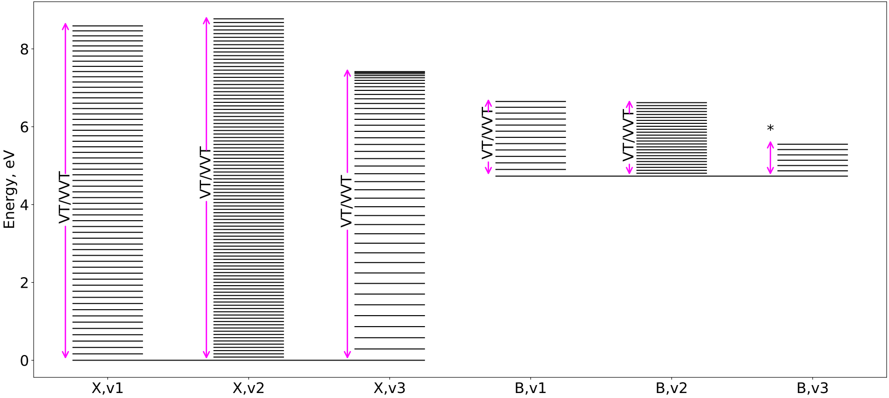

IVT

Including inter-mode (IVT) energy exchanges

$$P_{\mathsf{IVT}} = P_{\mathsf{VT}}(\mathsf{v}_i \to 0) P_{\mathsf{VT}}(0 \to \mathsf{v}_f)$$

v_i and v_f are from different vibrational modes.

The product of probabilities makes $P_{\mathsf{IVT}} \to 0$ when v_i or v_f grows

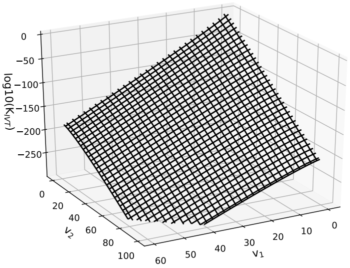

$\log_{10}(K_{\mathsf{IVT}})$ at 5,000 K

Model Schematic

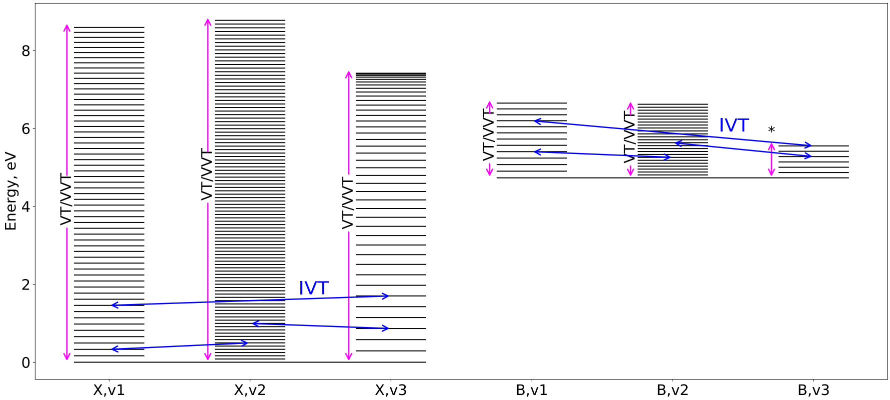

Singlet-Triplet Interaction

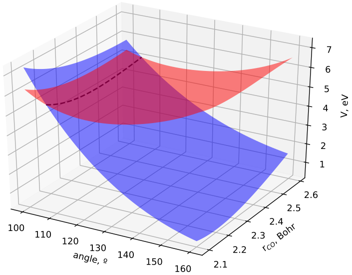

Including the interaction between $CO_2(X)$ and $CO_2(B)$.

- The ground and triplet state cross
- The crossing point cannot be accurately determined
- Approximate region indicates the crossing is dominated by the ground state bending mode

Crossing is modeled through Rosen-Zener theory.

*Upper figure is illustrative

Singlet-Triplet Interaction

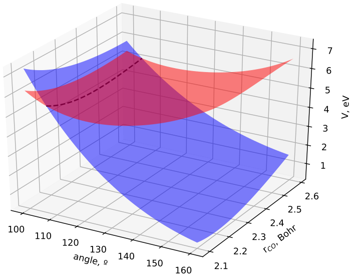

Including the interaction between $CO_2(X)$ and $CO_2(B)$.

- The ground and triplet state cross
- The crossing point cannot be accurately determined
- Approximate region indicates the crossing is dominated by the ground state bending mode

Crossing is modeled through Rosen-Zener theory.

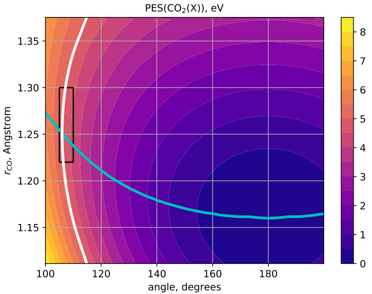

*Upper figure is illustrative

Model Schematic

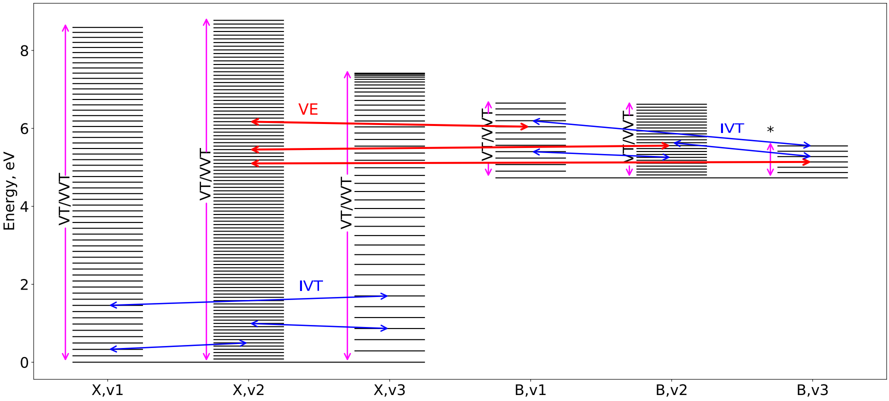

Pathways to dissociation

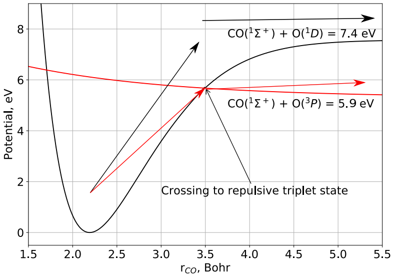

*Red line empirical potential

Three pathways for dissociation

- Ladder climbing dissociation is possible for the ground and triplet state

Pathways to dissociation

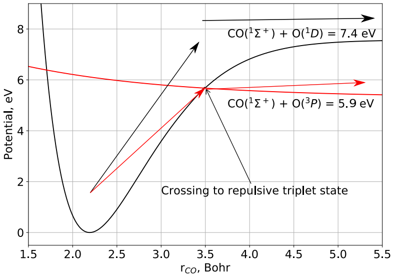

*Red line empirical potential

Three pathways for dissociation

- Ladder climbing dissociation is possible for the ground and triplet state
- Another cross with a repulsive configuration of a triplet state occurs at 5.85 eV

Pathways to dissociation

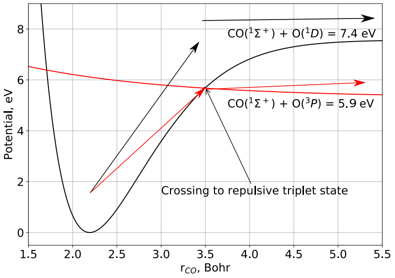

*Red line empirical potential

Three pathways for dissociation

- Ladder climbing dissociation is possible for the ground and triplet state
- Another cross with a repulsive configuration of a triplet state occurs at 5.85 eV
- First two paths can be modelled using FHO, the third one through Rosen-Zener theory

Model Schematic

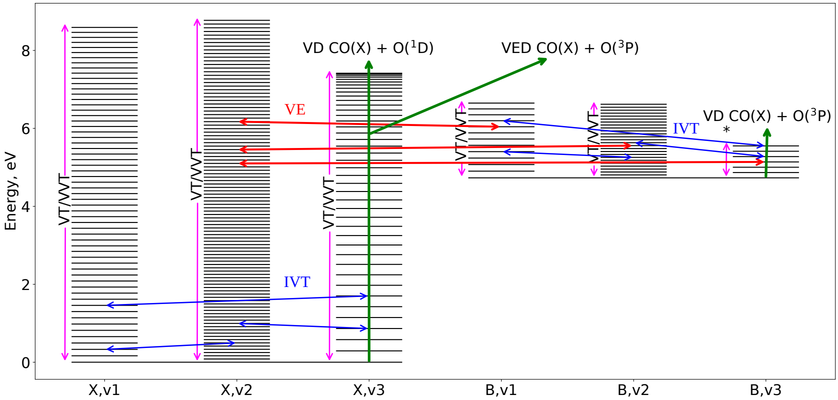

Exchange Reactions

The exchange reaction $CO_2 + O \longleftrightarrow CO + O_2$ should be included. Dean (1973) observed increased CO_2 dissociation with increased presence of O atoms.

Exchange Reactions

The exchange reaction $CO_2 + O \longleftrightarrow CO + O_2$ should be included. Dean (1973) observed increased CO_2 dissociation with increased presence of O atoms.

- No available state to state reaction rates
- Macroscopic rates available in literature
- Redistribution of macroscopic rate is performed with J. Annaloro (2013) method using CO_2 ground state only

Exchange Reactions

The exchange reaction $CO_2 + O \longleftrightarrow CO + O_2$ should be included. Dean (1973) observed increased CO_2 dissociation with increased presence of O atoms.

- No available state to state reaction rates
- Macroscopic rates available in literature
- Redistribution of macroscopic rate is performed with J. Annaloro (2013) method using CO_2 ground state only

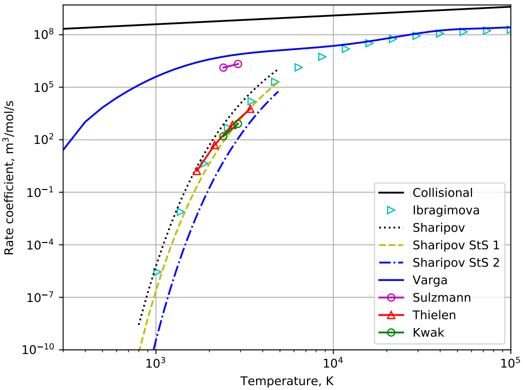

Exchange Reactions

The exchange reaction $CO_2 + O \longleftrightarrow CO + O_2$ should be included. Dean (1973) observed increased CO_2 dissociation with increased presence of O atoms.

- No available state to state reaction rates
- Macroscopic rates available in literature
- Redistribution of macroscopic rate is performed with J. Annaloro (2013) method using CO_2 ground state only

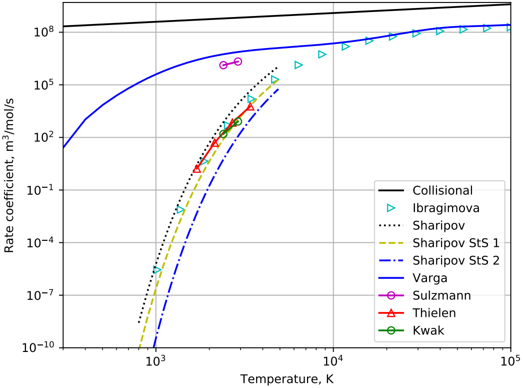

A set of state to state $CO_2(X,v) + O \longleftrightarrow CO + O_2$ reaction rates is included.

Other Reactions

The set of reactions in Cruden *et al.* (2018) is also included.

Reaction	A (m^3/mol/s)	n	E_a (K)
$CO + M \longleftrightarrow C + O + M$	7.99E+32	-5.50	1.29E+5
$C_2 + O \longleftrightarrow CO + C$	3.61E+08	0.00	0.0E+0
$C_2 + M \longleftrightarrow C + C + M$	1.82E+09	0.00	6.40E+4
$CO + O \longleftrightarrow C + O_2$	3.90E+07	-0.18	6.92E+4
$O_2 + M \longleftrightarrow O + O + M$	1.20E+08	0.00	5.42E+4
$C + e^- \longleftrightarrow C^+ + e^- + e^-$	3.70E+25	-3.00	1.30E+5
$O + e^- \longleftrightarrow O^+ + e^- + e^-$	3.90E+27	-3.78	1.58E+5
$CO + e^- \longleftrightarrow CO^+ + e^- + e^-$	4.50E+08	2.75	1.63E+5
$O_2 + e^- \longleftrightarrow {O_2}^+ + e^- + e^-$	2.19E+04	1.16	1.30E+5
$C + O \longleftrightarrow CO^+ + e^-$	8.80E+02	1.00	3.31E+4
$CO + C^+ \longleftrightarrow CO^+ + C$	1.10E+07	0.00	3.14E+4
$O + O \longleftrightarrow {O_2}^+ + e^-$	7.10E-04	2.70	8.06E+4
$O_2 + C^+ \longleftrightarrow {O_2}^+ + C$	1.00E+07	0.00	9.40E+3
${O_2}^+ + O \longleftrightarrow O_2 + O^+$	2.19E+04	1.16	1.30E+5

Set of reactions calibrated against EAST experiments

Summary

Name	Type	#Reac.
$CO_2(X,v'_1) + M \leftrightarrow CO_2(X,v''_1) + M$	VT	1770
$CO_2(X,v'_2) + M \leftrightarrow CO_2(X,v''_2) + M$	VT	5050
$CO_2(X,v'_3) + M \leftrightarrow CO_2(X,v''_3) + M$	VT	861
$CO_2(X,v'_1) + CO_2(X,v'_1) \leftrightarrow CO_2(X,v'_1+1) + CO_2(X,v'_1-1)$	VVT	58
$CO_2(X,v'_2) + CO_2(X,v'_2) \leftrightarrow CO_2(X,v'_2+1) + CO_2(X,v'_2-1)$	VVT	99
$CO_2(X,v'_3) + CO_2(X,v'_3) \leftrightarrow CO_2(X,v'_3+1) + CO_2(X,v'_3-1)$	VVT	41
$CO_2(X,v'_1) + M \leftrightarrow CO_2(X,v''_2) + M$	IVT	5900
$CO_2(X,v'_1) + M \leftrightarrow CO_2(X,v''_3) + M$	IVT	2478
$CO_2(X,v'_2) + M \leftrightarrow CO_2(X,v''_3) + M$	IVT	4200
$CO_2(B,v'_1) + M \leftrightarrow CO_2(B,v''_1) + M$	VT	78
$CO_2(B,v'_2) + M \leftrightarrow CO_2(B,v''_2) + M$	VT	325
$CO_2(B,v'_3) + M \leftrightarrow CO_2(B,v''_3) + M$	VT	21
$CO_2(B,v'_1) + CO_2(B,v'_1) \leftrightarrow CO_2(B,v'_1+1) + CO_2(B,v'_1-1)$	VVT	11
$CO_2(B,v'_2) + CO_2(B,v'_2) \leftrightarrow CO_2(B,v'_2+1) + CO_2(B,v'_2-1)$	VVT	24
$CO_2(B,v'_3) + CO_2(B,v'_3) \leftrightarrow CO_2(B,v'_3+1) + CO_2(B,v'_3-1)$	VVT	6
$CO_2(B,v'_1) + M \leftrightarrow CO_2(B,v''_2) + M$	IVT	300
$CO_2(B,v'_1) + M \leftrightarrow CO_2(B,v''_3) + M$	IVT	84
$CO_2(B,v'_2) + M \leftrightarrow CO_2(B,v''_3) + M$	IVT	175
$CO_2(X,v'_2) + M \leftrightarrow CO_2(B,v''_1) + M$	VE	103
$CO_2(X,v'_2) + M \leftrightarrow CO_2(B,v''_2) + M$	VE	311
$CO_2(X,v'_2) + M \leftrightarrow CO_2(B,v''_3) + M$	VE	163
$CO_2(X,v'_3) + M \leftrightarrow CO + O(^1D) + M$	VD	42
$CO_2(X,v'_3) + M \leftrightarrow CO + O(^3P) + M$	VD	42
$CO_2(B,v'_3) + M \leftrightarrow CO + O(^3P) + M$	VD	7
$CO_2(X,v'_{1,2,3}) + O(^3P) \leftrightarrow CO + O_2$	Zeldov.	201
$CO_2(X,v'_{1,2,3}) + C \leftrightarrow CO + CO$	Zeldov.	201
$O(^1D) + M \leftrightarrow O(^3P) + M$	Quench.	4

A total of 22566 reactions (with only extreme states)

Test Cases

Case 1: Isothermal

0D Isotherm. in pure CO_2 (no dissociation), $T_v = 300$ K and 2 kPa, $T_g = 10{,}000$ K

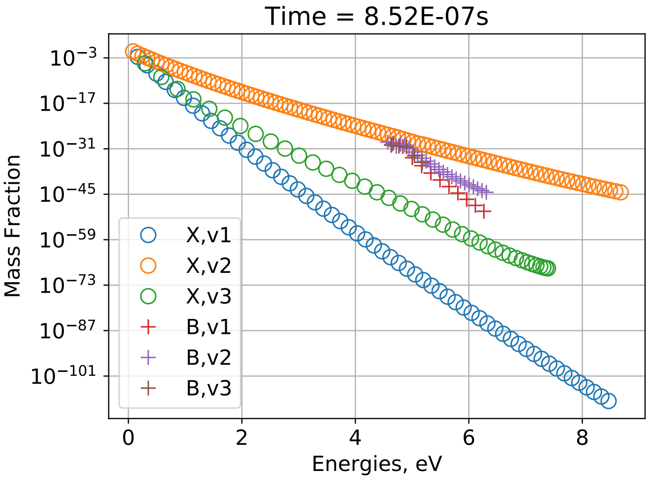

Case 1: Isothermal

0D Isotherm. in pure CO_2 (no dissociation), $T_v = 300$ K and 2 kPa, $T_g = 10{,}000$ K

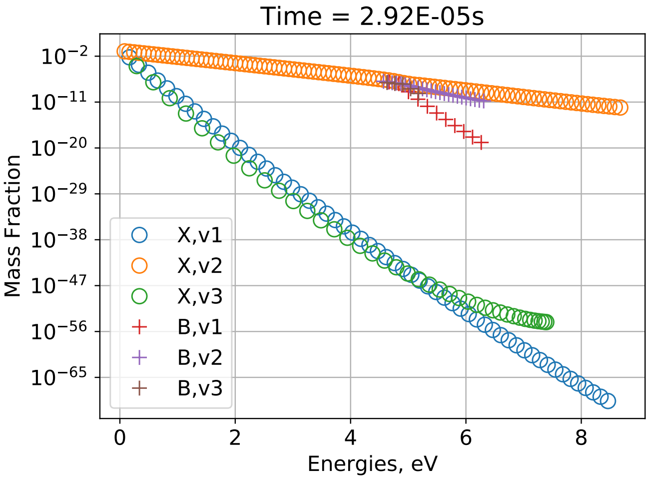

Case 1: Isothermal

0D Isotherm. in pure CO_2 (no dissociation), $T_v = 300$ K and 2 kPa, $T_g = 10{,}000$ K

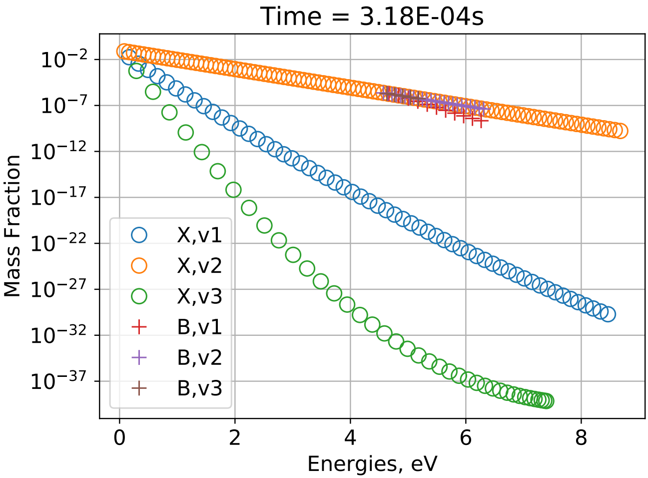

Case 1: Isothermal

0D Isotherm. in pure CO_2 (no dissociation), $T_v = 300$ K and 2 kPa, $T_g = 10{,}000$ K

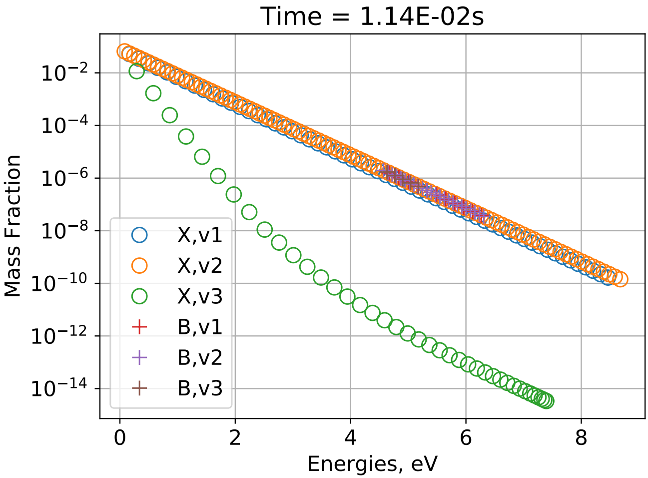

Case 2: Dissociation

0D pure CO_2 at 300K and 2kPa suddenly heated to 10,000K

Case 2: Dissociation

0D pure CO_2 at 300K and 2kPa suddenly heated to 10,000K

- Temperature (Boltzmann fitted) evolution indicates internal modes follow isothermal case
- $CO_2 + O \longleftrightarrow CO + O_2$ dominates CO_2 decomposition
- O atoms are created through $CO_2 + M \longleftrightarrow CO + O + M$ which then accelerate the $CO_2 + O$ collision

Case 2: Dissociation

0D pure CO_2 at 300K and 2kPa suddenly heated to 10,000K

- Temperature (Boltzmann fitted) evolution indicates internal modes follow isothermal case
- $CO_2 + O \longleftrightarrow CO + O_2$ dominates CO_2 decomposition
- O atoms are created through $CO_2 + M \longleftrightarrow CO + O + M$ which then accelerate the $CO_2 + O$ collision

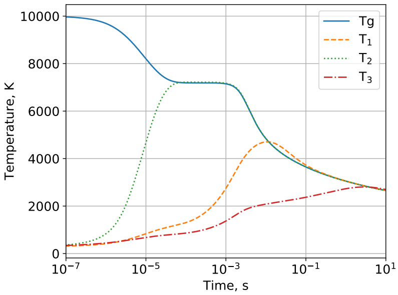

0D pure CO_2 at 300K and 2kPa suddenly heated to 10,000K

- Temperature (Boltzmann fitted) evolution indicates internal modes follow isothermal case
- $CO_2 + O \longleftrightarrow CO + O_2$ dominates CO_2 decomposition
- O atoms are created through $CO_2 + M \longleftrightarrow CO + O + M$ which then accelerate the $CO_2 + O$ collision

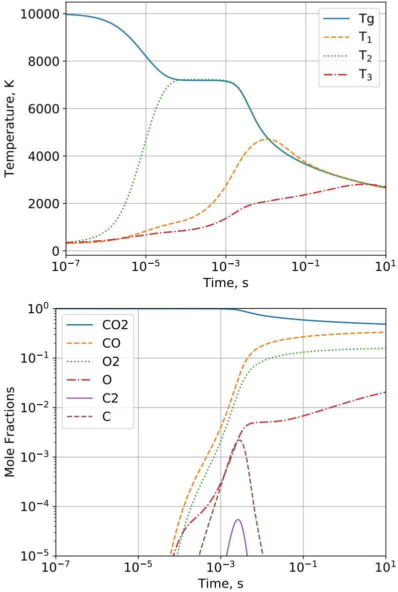

Case 3: Recombination

Dissociated 1000K CO_2 gas at 1 bar

Case 3: Recombination

Dissociated 1000K CO_2 gas at 1 bar

- Analogous to a recombination exp.
- Typical recomb. time scale in exp. measurements is *ms*
- Depending on the chosen $CO_2 + O \longleftrightarrow CO + O_2$ rate, recombination occurs at 10^5 or 10^{-3} seconds

Case 3: Recombination

Dissociated 1000K CO_2 gas at 1 bar

- Analogous to a recombination exp.
- Typical recomb. time scale in exp. measurements is *ms*
- Depending on the chosen $CO_2 + O \longleftrightarrow CO + O_2$ rate, recombination occurs at 10^5 or 10^{-3} seconds

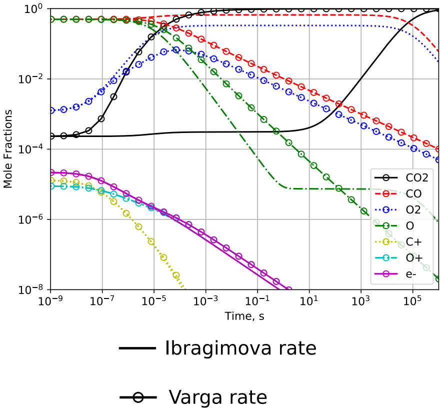

Case 4: CO_2 Decomposition Time

- Shots in VUT-1 shock tube at MIPT (Moscow, Russia)
- ESA TRP *CFD validation in a CO_2 environment*, 2008.
- VUV lamp used to assess relative concentration of $CO_2(X)$ by absorption

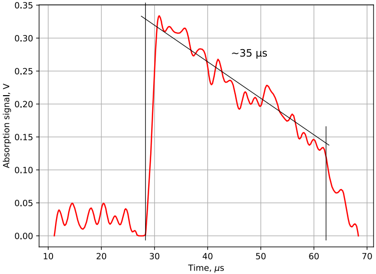

Case 4: CO_2 Decomposition Time

- Shots in VUT-1 shock tube at MIPT (Moscow, Russia)
- ESA TRP *CFD validation in a CO_2 environment*, 2008.
- VUV lamp used to assess relative concentration of $CO_2(X)$ by absorption

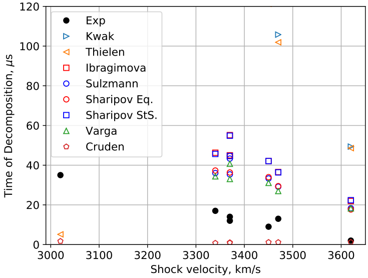

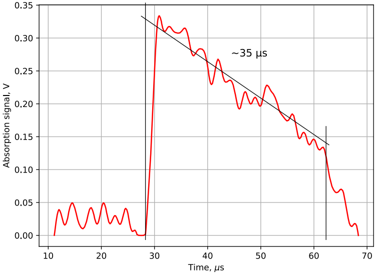

- Typical time scale 1-40 μs
- Macroscopic model always predicts $< 2\mu$s
- StS model provides correct shock-velocity trends and overpredicts decomposition times by 50-100%

Radiation

CDSD4000 will be used to refit a vibrationally specific CO_2 IR database

Dubbed CDSDv, this database will feature:

CO_2 IR Radiation Modelling

CDSD4000 will be used to refit a vibrationally specific CO_2 IR database

Dubbed CDSDv, this database will feature:

- Separation between rotational and vibrational modes

CDSD4000 will be used to refit a vibrationally specific CO_2 IR database

Dubbed CDSDv, this database will feature:

- Separation between rotational and vibrational modes
- Can be coupled to kinetic solver

$$\frac{dN_i}{dt} = \sum_j K_{ij} N_i N_j - \sum_j K_{ji} N_j N_i - \sum_j A_{ij} N_i$$

CO_2 IR Radiation Modelling

CDSD4000 will be used to refit a vibrationally specific CO_2 IR database

Dubbed CDSDv, this database will feature:

- Separation between rotational and vibrational modes
- Can be coupled to kinetic solver

$$\frac{dN_i}{dt} = \sum_j K_{ij} N_i N_j - \sum_j K_{ji} N_j N_i - \sum_j A_{ij} N_i$$

- Reconstruction of ro-vibrational data

CO_2 IR Radiation Modelling

CDSD4000 will be used to refit a vibrationally specific CO_2 IR database

Dubbed CDSDv, this database will feature:

- Separation between rotational and vibrational modes
- Can be coupled to kinetic solver

$$\frac{dN_i}{dt} = \sum_j K_{ij} N_i N_j - \sum_j K_{ji} N_j N_i - \sum_j A_{ij} N_i$$

- Reconstruction of ro-vibrational data
- Will lose detail: not suitable for detailed spectroscopy, perturbations will not be accounted for.

Level Database

Fit ro-vibrational energy levels:

$$\boxed{E_{vJ} = G_v + B_v[J(J+1)] - D_v[J(J+1)]^2 + H_v[J(J+1)]^3}$$

Level Database

Fit ro-vibrational energy levels:

$$E_{vJ} = G_v + B_v[J(J+1)] - D_v[J(J+1)]^2 + H_v[J(J+1)]^3$$

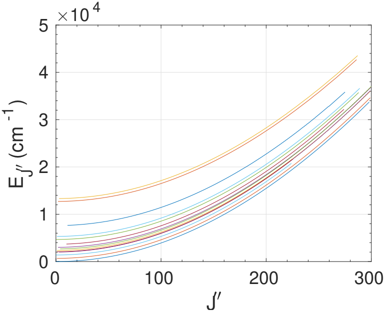

Fit ro-vibrational energy levels:

$$E_{vJ} = G_v + B_v[J(J+1)] - D_v[J(J+1)]^2 + H_v[J(J+1)]^3$$

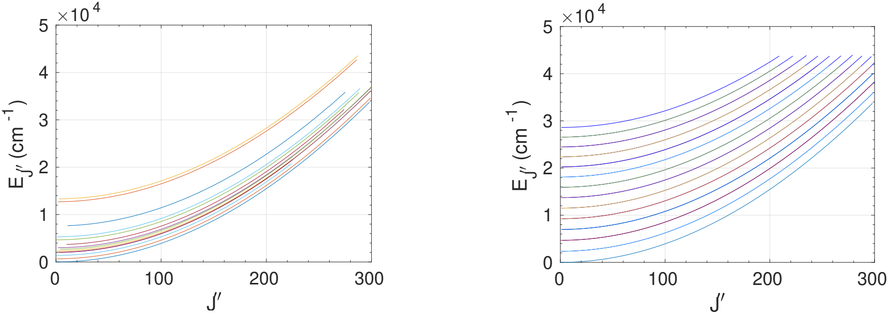

Level Database

Fit ro-vibrational energy levels:

$$E_{vJ} = G_v + B_v[J(J+1)] - D_v[J(J+1)]^2 + H_v[J(J+1)]^3$$

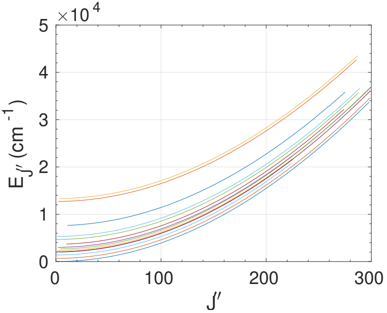

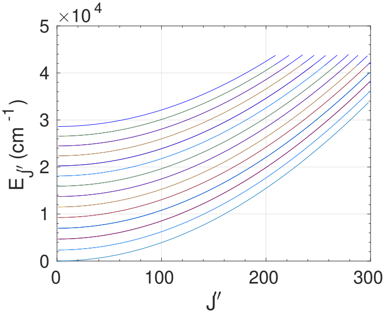

Extrapolation of J to 300 (or 301) or to E_{diss}.

We now have a levels database.

Fitting Transitions

$$A_{v''}^{v'} \times F_{J',J''} = \frac{A_{v''J''}^{v'J'}}{S_{l''J''}^{l'J'}}$$

- $A_{v''}^{v'}$ –Vibrational Einstein coefficients
- $F_{J',J''}$ –Herman-Wallis factors
- $A_{v''J''}^{v'J'}$ –Ro-vibrational Einstein coefficients
- $S_{l''J''}^{l'J'}$ –Hönl-London factors

- RHS is obtained through reading databases
- LHS is a polynomial expansion

Fitting Transitions

$$\boxed{A^{v'}_{v''} \times F_{J',J''} = \frac{A^{v'J'}_{v''J''}}{S^{l'J'}_{l''J''}}}$$

- $A^{v'}_{v''}$ –Vibrational Einstein coefficients
- $F_{J',J''}$ –Herman-Wallis factors
- $A^{v'J'}_{v''J''}$ –Ro-vibrational Einstein coefficients
- $S^{l'J'}_{l''J''}$ –Hönl-London factors

- RHS is obtained through reading databases
- LHS is a polynomial expansion
- Ro-vibrational transitions have branches and polynomial coefficients are shared

Fitting Transitions

$$\boxed{A^{v'}_{v''} \times F_{J',J''} = \frac{A^{v'J'}_{v''J''}}{S^{l'J'}_{l''J''}}}$$

- $A^{v'}_{v''}$ –Vibrational Einstein coefficients
- $F_{J',J''}$ –Herman-Wallis factors
- $A^{v'J'}_{v''J''}$ –Ro-vibrational Einstein coefficients
- $S^{l'J'}_{l''J''}$ –Hönl-London factors

- RHS is obtained through reading databases
- LHS is a polynomial expansion
- Ro-vibrational transitions have branches and polynomial coefficients are shared

Each transition is fitted for every branch “simultaneously"

Transition Fitting

Some examples of transition fitting.

- Transitions 00011→00001 and 01111→01101 (e and f)
- Perturbed data was removed prior to fitting.
- Data was truncated at convenient J

Transition Fitting

Some examples of transition fitting.

- Transitions 00011→00001 and 01111→01101 (e and f)
- Perturbed data was removed prior to fitting.
- Data was truncated at convenient J

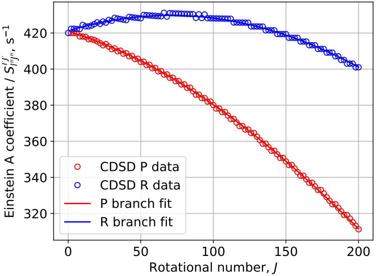

Transition Fitting

Some examples of transition fitting.

- Transitions 00011→00001 and 01111→01101 (e and f)
- Perturbed data was removed prior to fitting.
- Data was truncated at convenient J

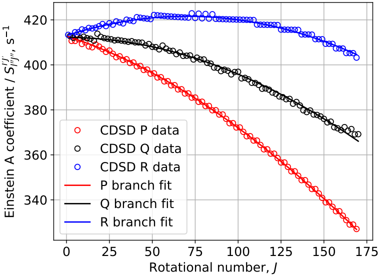

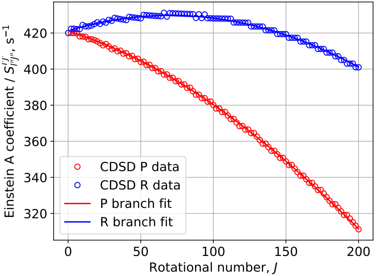

Transition Fitting

Some examples of transition fitting.

- Transitions 00011→00001 and 01111→01101 (e and f)
- Perturbed data was removed prior to fitting.
- Data was truncated at convenient J

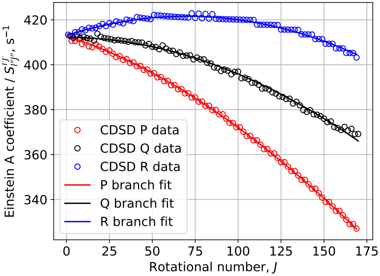

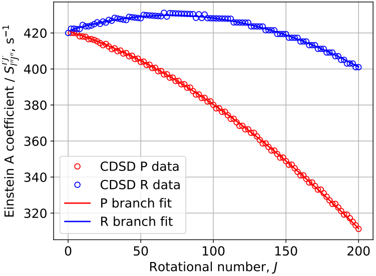

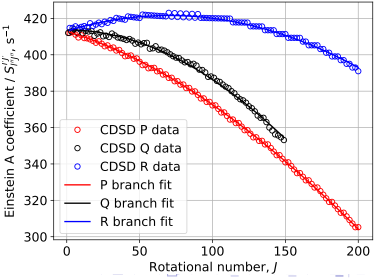

Reconstruction of Einstein Coefficients

Reconstructed Einstein coefficients of transitions 00011→00001 (top) and 01111→01101 (bottom).

Comparison with CDSD4000 and HITRAN values.

Perturbed data is not reproduced and does not affect fitting

Reconstruction of Einstein Coefficients

Reconstructed Einstein coefficients of transitions 00011→00001 (top) and 01111→01101 (bottom).

Comparison with CDSD4000 and HITRAN values.

Perturbed data is not reproduced and does not affect fitting

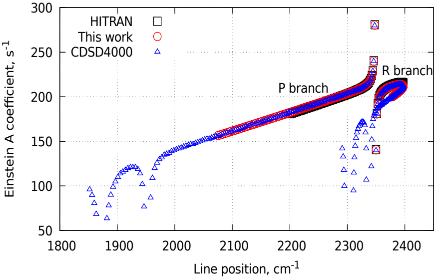

Reconstruction of Einstein Coefficients

Reconstructed Einstein coefficients of transitions 00011→00001 (top) and 01111→01101 (bottom).

Comparison with CDSD4000 and HITRAN values.

Perturbed data is not reproduced and does not affect fitting

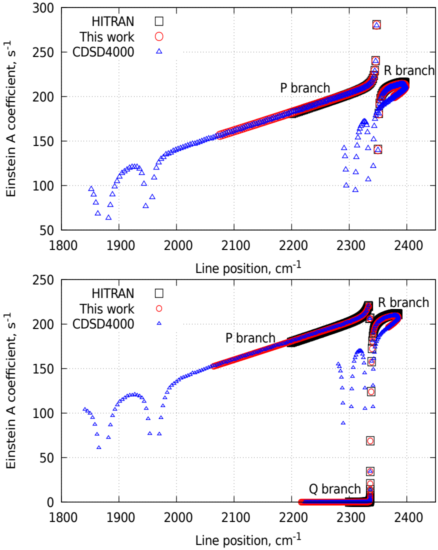

Lorentz Broadening

In CDSD4000:

- Semi empirical expressions
- Only Air and Self broadening
- From reference p and T values

Lorentz Broadening

In CDSD4000:

- Semi empirical expressions
- Only Air and Self broadening
- From reference p and T values

In CDSDv:

- Generalized expressions, effect dependant
- Can be used for any mixture

Lorentz Broadening

In CDSD4000:

- Semi empirical expressions
- Only Air and Self broadening
- From reference p and T values

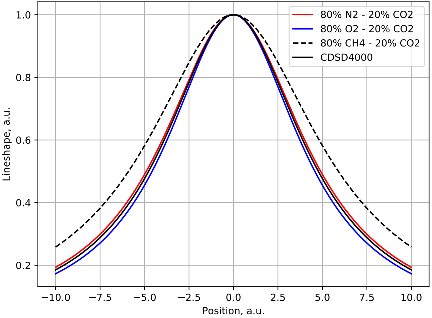

In CDSDv:

- Generalized expressions, effect dependant
- Can be used for any mixture

Lorentz Broadening

In CDSD4000:

- Semi empirical expressions
- Only Air and Self broadening
- From reference p and T values

In CDSDv:

- Generalized expressions, effect dependant
- Can be used for any mixture

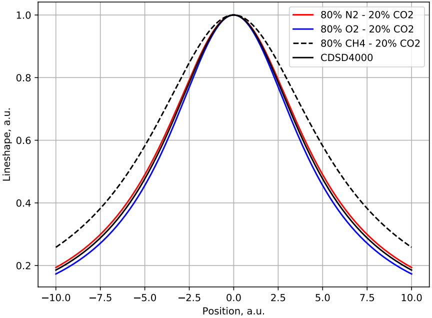

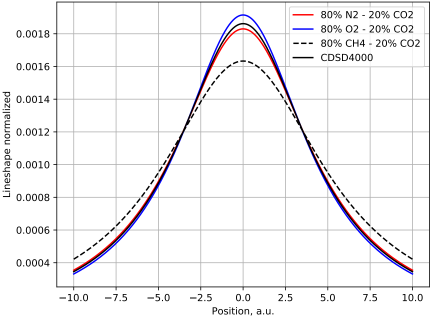

$T = 298$ K and $p = 50$ atm

Absorption Coefficient

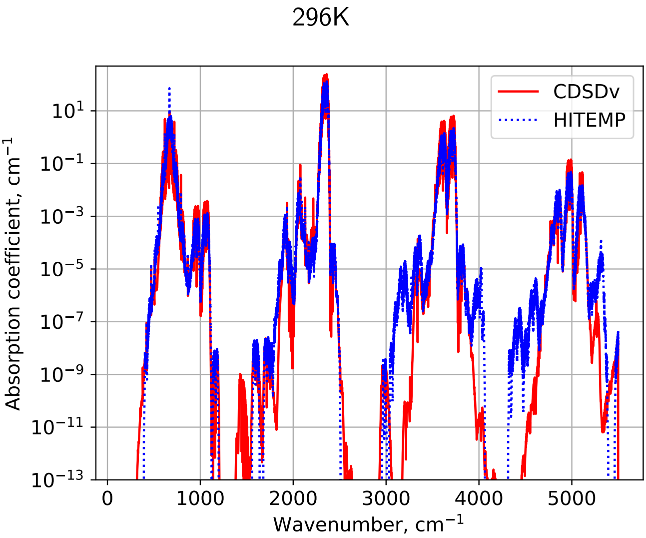

Absorption Coefficient

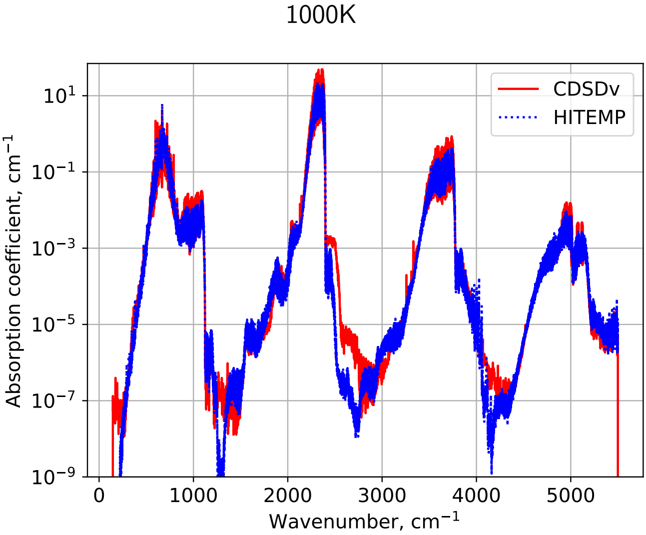

Absorption Coefficient

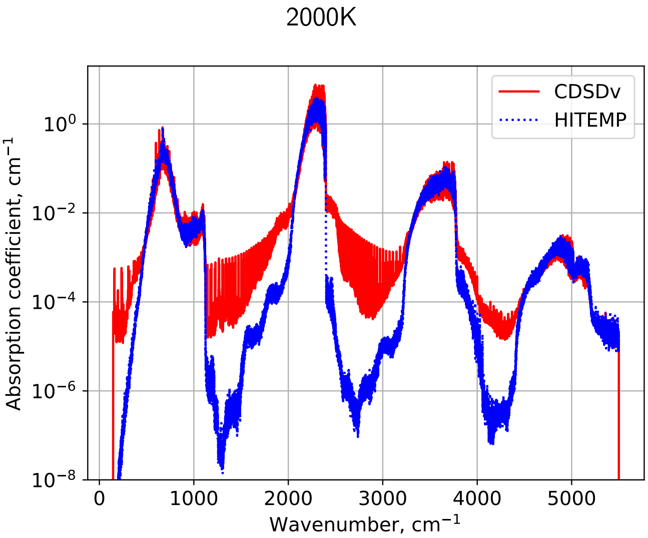

Absorption Coefficient

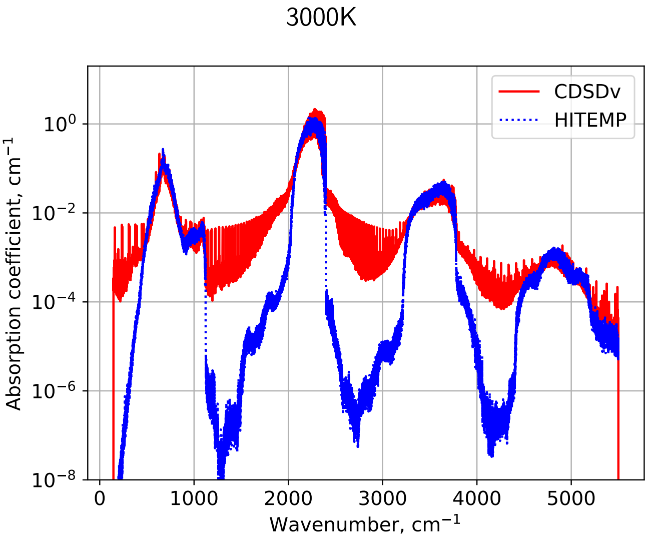

Test Cases

Case 1: JAXA Mars Entry

Measurements of IR radiation were carried out in JAXA facility by Takaynagi *et al.* (2018). Pannier and Laux (2019) performed a numerical analysis repeated here.

Case 1: JAXA Mars Entry

Measurements of IR radiation were carried out in JAXA facility by Takaynagi *et al.* (2018). Pannier and Laux (2019) performed a numerical analysis repeated here.

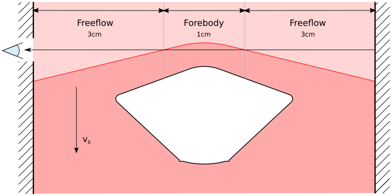

- 4.3 μm region
- Line of sight 7 cm long simplified into 3 zones
- 1st and 3rd cell are free flow zones, low pressure, non-eq.
- 2nd cell is the forebody cell, high pressure and temperature, no CO_2

Case 1: JAXA Mars Entry

Measurements of IR radiation were carried out in JAXA facility by Takaynagi *et al.* (2018). Pannier and Laux (2019) performed a numerical analysis repeated here.

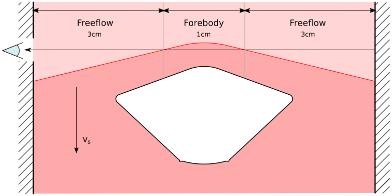

- 4.3 μm region
- Line of sight 7 cm long simplified into 3 zones
- 1st and 3rd cell are free flow zones, low pressure, non-eq.
- 2nd cell is the forebody cell, high pressure and temperature, no CO_2

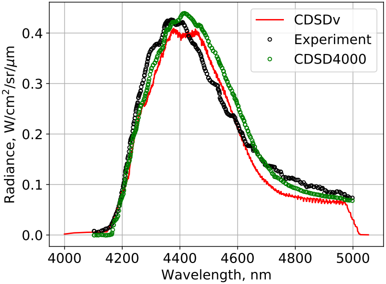

Very good agreement

Case 2: EAST MSL Entry

Campaign at EAST - Mars Science Laboratory conditions

- Shock at 3.69 km/s
- 1 Torr, 97% CO_2
- 4.3 μm spectral region
- Peak Temperature at 3050 K

Simulation profile kindly shared by B. Cruden.

Case 2: EAST MSL Entry

Campaign at EAST - Mars Science Laboratory conditions

- Shock at 3.69 km/s
- 1 Torr, 97% CO_2
- 4.3 μm spectral region
- Peak Temperature at 3050 K

Simulation profile kindly shared by B. Cruden.

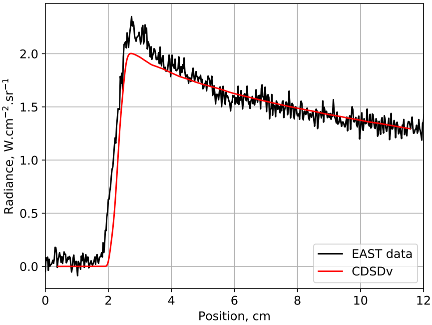

Case 3: Atmospheric Plasma Torch

CO_2 Atmospheric plasma torch at 1,000–5,000K, work of Depraz *et al.* (2012)

- 2.7 and 4.3 μm regions probed
- Measurements at $h = 6,\ 20$ mm
- Torch radial profile is divided into 10 cells

Radiative Transfer with CDSDv + CO in the central chord: line of sight is taken as the full diameter of the torch.

Case 3: Atmospheric Plasma Torch

CO_2 Atmospheric plasma torch at 1,000–5,000K, work of Depraz *et al.* (2012)

- 2.7 and 4.3 μm regions probed
- Measurements at $h = 6, 20$ mm
- Torch radial profile is divided into 10 cells

Radiative Transfer with CDSDv + CO in the central chord: line of sight is taken as the full diameter of the torch.

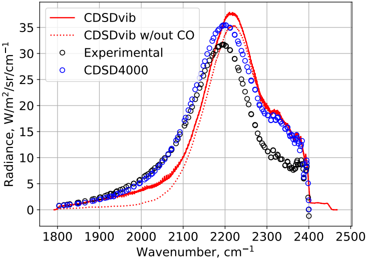

6 mm, 4.3μm

CO_2 Atmospheric plasma torch at 1,000–5,000K, work of Depraz *et al.* (2012)

- 2.7 and 4.3 μm regions probed
- Measurements at $h = 6, 20$ mm
- Torch radial profile is divided into 10 cells

Radiative Transfer with CDSDv + CO in the central chord: line of sight is taken as the full diameter of the torch.

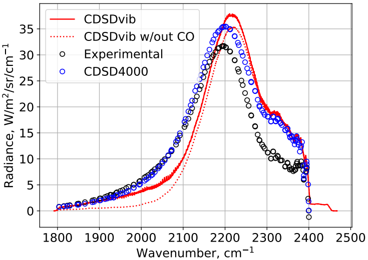

6 mm, 4.3μm

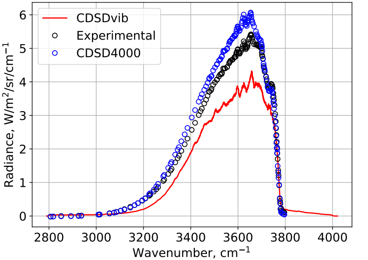

6 mm, 2.7μm

Conclusions

Accomplishments

- A more physically consistent approach to CO_2 dissociation has been presented

Accomplishments

- A more physically consistent approach to CO_2 dissociation has been presented
  - Step-up from SSH-based models

Accomplishments

- A more physically consistent approach to CO_2 dissociation has been presented
  - Step-up from SSH-based models
  - Inclusion of $^3B_2$ state

Accomplishments

- A more physically consistent approach to CO_2 dissociation has been presented
  - Step-up from SSH-based models
  - Inclusion of $^3B_2$ state
  - Displayed physically consistent though not 100% predictive results

Accomplishments

- A more physically consistent approach to CO_2 dissociation has been presented
  - Step-up from SSH-based models
  - Inclusion of $^3B_2$ state
  - Displayed physically consistent though not 100% predictive results
  - Lots of room for improvement

Accomplishments

- A more physically consistent approach to CO_2 dissociation has been presented
  - Step-up from SSH-based models
  - Inclusion of $^3B_2$ state
  - Displayed physically consistent though not 100% predictive results
  - Lots of room for improvement

- A CO_2 IR radiation database was presented

Accomplishments

- A more physically consistent approach to CO_2 dissociation has been presented
  - Step-up from SSH-based models
  - Inclusion of $^3B_2$ state
  - Displayed physically consistent though not 100% predictive results
  - Lots of room for improvement

- A CO_2 IR radiation database was presented
  - Refitting method is universal

Accomplishments

- A more physically consistent approach to CO_2 dissociation has been presented
  - Step-up from SSH-based models
  - Inclusion of $^3B_2$ state
  - Displayed physically consistent though not 100% predictive results
  - Lots of room for improvement

- A CO_2 IR radiation database was presented
  - Refitting method is universal
  - Broadening calculation is more flexible

Accomplishments

- A more physically consistent approach to CO_2 dissociation has been presented
  - Step-up from SSH-based models
  - Inclusion of $^3B_2$ state
  - Displayed physically consistent though not 100% predictive results
  - Lots of room for improvement

- A CO_2 IR radiation database was presented
  - Refitting method is universal
  - Broadening calculation is more flexible
  - In the 4.3 μm region, reduction from 81M to 5M lines

Accomplishments

- A more physically consistent approach to CO_2 dissociation has been presented
  - Step-up from SSH-based models
  - Inclusion of $^3B_2$ state
  - Displayed physically consistent though not 100% predictive results
  - Lots of room for improvement

- A CO_2 IR radiation database was presented
  - Refitting method is universal
  - Broadening calculation is more flexible
  - In the 4.3 μm region, reduction from 81M to 5M lines
  - CDSDv database is 16.6 MB compared to CDSD4000 16 GB

Accomplishments

- A more physically consistent approach to CO_2 dissociation has been presented
  - Step-up from SSH-based models
  - Inclusion of $^3B_2$ state
  - Displayed physically consistent though not 100% predictive results
  - Lots of room for improvement

- A CO_2 IR radiation database was presented
  - Refitting method is universal
  - Broadening calculation is more flexible
  - In the 4.3 μm region, reduction from 81M to 5M lines
  - CDSDv database is 16.6 MB compared to CDSD4000 16 GB
  - Reasonable agreement with experiments and calculations

Accomplishments

- A more physically consistent approach to CO_2 dissociation has been presented
  - Step-up from SSH-based models
  - Inclusion of $^3B_2$ state
  - Displayed physically consistent though not 100% predictive results
  - Lots of room for improvement
- A CO_2 IR radiation database was presented
  - Refitting method is universal
  - Broadening calculation is more flexible
  - In the $4.3\ \mu$m region, reduction from 81M to 5M lines
  - CDSDv database is 16.6 MB compared to CDSD4000 16 GB
  - Reasonable agreement with experiments and calculations
  - Significant performance enhancement

Further work

Kinetics

Further work

Kinetics

- Different collision partners

Further work

Kinetics

- Different collision partners
- Improve intermode transition rates

Further work

Kinetics

- Different collision partners
- Improve intermode transition rates
- Inclusion of radiative processes

Further work

Kinetics

- Different collision partners
- Improve intermode transition rates
- Inclusion of radiative processes
- Uncertainty $CO_2 + O \longleftrightarrow CO + O_2$

Further work

Kinetics

- Different collision partners
- Improve intermode transition rates
- Inclusion of radiative processes
- Uncertainty $CO_2 + O \longleftrightarrow CO + O_2$
- Reduced order modelling

Further work

Kinetics

- Different collision partners
- Improve intermode transition rates
- Inclusion of radiative processes
- Uncertainty $CO_2 + O \longleftrightarrow CO + O_2$
- Reduced order modelling
- **Experimental validation**

Radiation

Further work

Kinetics

- Different collision partners
- Improve intermode transition rates
- Inclusion of radiative processes
- Uncertainty $CO_2 + O \longleftrightarrow CO + O_2$
- Reduced order modelling
- **Experimental validation**

Radiation

- Adding a C/J or $C/(J+1)$ term on Herman-Wallis expressions

Further work

Kinetics

- Different collision partners
- Improve intermode transition rates
- Inclusion of radiative processes
- Uncertainty $CO_2 + O \longleftrightarrow CO + O_2$
- Reduced order modelling
- **Experimental validation**

Radiation

- Adding a C/J or $C/(J+1)$ term on Herman-Wallis expressions
- Add more transitions, 2.7 and 4.3 μm regions

Further work

Kinetics

- Different collision partners
- Improve intermode transition rates
- Inclusion of radiative processes
- Uncertainty $CO_2 + O \longleftrightarrow CO + O_2$
- Reduced order modelling
- **Experimental validation**

Radiation

- Adding a C/J or $C/(J+1)$ term on Herman-Wallis expressions
- Add more transitions, 2.7 and 4.3 μm regions
- Apply CDSDv to cases with different mixtures of gases

Further work

Kinetics

- Different collision partners
- Improve intermode transition rates
- Inclusion of radiative processes
- Uncertainty $CO_2 + O \longleftrightarrow CO + O_2$
- Reduced order modelling
- **Experimental validation**

Radiation

- Adding a C/J or $C/(J+1)$ term on Herman-Wallis expressions
- Add more transitions, 2.7 and 4.3 μm regions
- Apply CDSDv to cases with different mixtures of gases
- Fitting of CDSDv to emission spectra

Final Remarks

There is still a lot of multi-disciplinary work to be done. It is my hope this work can be used as a reference point for further developments.

Final Remarks

There is still a lot of multi-disciplinary work to be done. It is my hope this work can be used as a reference point for further developments.

Would like to finish by acknowledging the role of other people in this work, some of whom are here present. Thank you

Final Remarks

There is still a lot of multi-disciplinary work to be done. It is my hope this work can be used as a reference point for further developments.

Would like to finish by acknowledging the role of other people in this work, some of whom are here present. Thank you

ipfn
INSTITUTO DE PLASMAS
E FUSÃO NUCLEAR

esa
European Space Agency

PD F FCT PhD PROGRAMMES

Partition Function

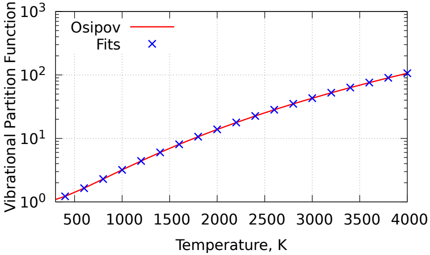

Partition function:

- Can be recovered from level database.
- Matches literature values for most of the temperature range.

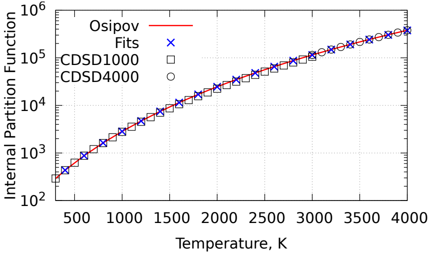

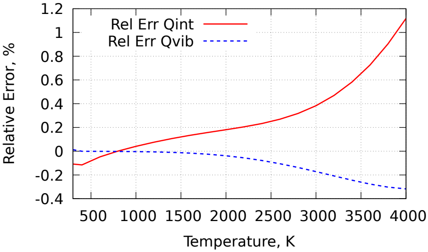

Osipov (2004), Tashkun *et al* (2003) and (2011)

Dissociation of CO_2

0D simulation, 3.69 km/s shock, 1 Torr in pure CO_2

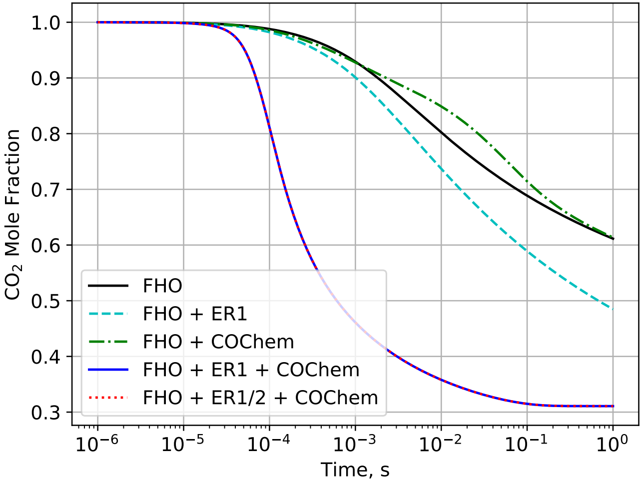

$CO + O_2 \longleftrightarrow CO_2 + O$

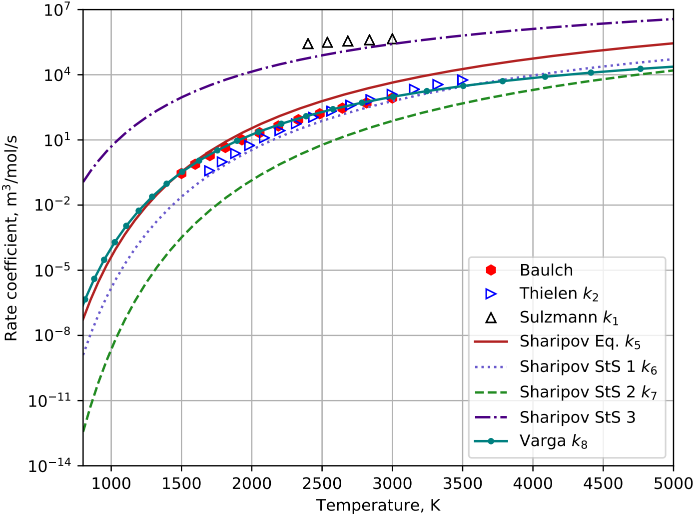

Note that I only performed inversion on Sharipov and Varga rates

More $CO + O_2 \longleftrightarrow CO_2 + O$

Rates already included:

- $CO_2(X,v) + O(^3P) \longleftrightarrow CO(X) + O_2(X)$
- $CO_2(X,v) + O(^1D) \longleftrightarrow CO(X) + O_2(X)$
- $CO_2(X,v) + C \longleftrightarrow CO(X) + CO(X)$

Other candidate rates to include:

- $CO(a) + O_2(X) \longleftrightarrow CO_2 + O(^3P)$
- $CO(X) + O_2(a) \longleftrightarrow CO_2 + O(^1D)$
- $O_2(a) + M \longleftrightarrow O_2(b) + M$
- $O_2(b) + O_2(X) \longleftrightarrow O_2(a) + O_2(a)$
- $CO(a) + CO \longleftrightarrow CO_2 + C$

IVT

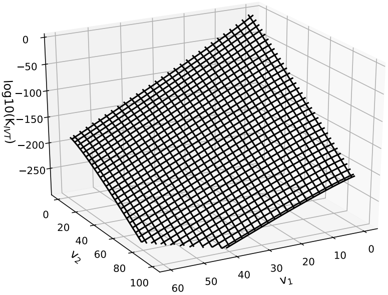

5,000 K

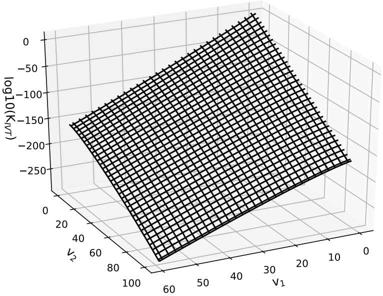

10,000 K

Radiative Power

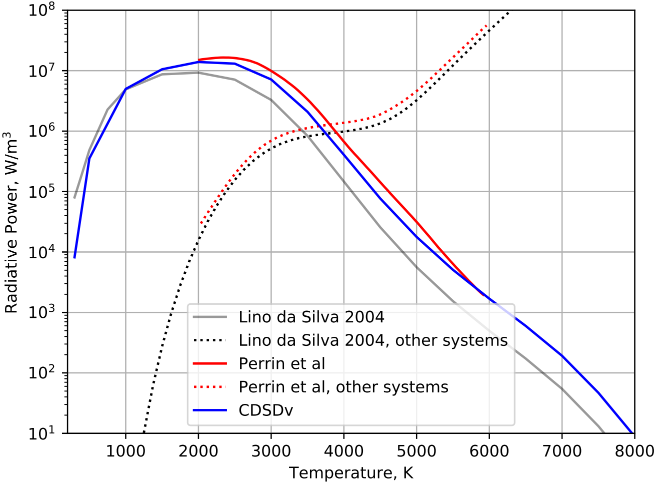

Performance

#	1		2	
Parameters	Tight		Lax	
Range	2100-2500		2000-2500	
Database	CDSDv	CDSD4000	CDSDv	CDSD4000
Time 1 (s)	30.98	85.18	20.11	174.95
Time 2 (s)	329.58	356.25	145.11	341.63
Time 3 (s)	2855.43	3891.64	1007.92	1773.45
Max RAM	446.3 MiB	3.830 GiB	607.75 MiB	7.985 GiB
# Lines	4,266,280	37,497,133	5,867,324	81,963,950

#	3		4	
Parameters	Lax		Tight	
Range	2100-2500		2000-2500	
Database	CDSDv	CDSD4000	CDSDv	CDSD4000
Time 1 (s)	17.09	65.53	39.95	181.62
Time 2 (s)	124.82	183.89	574.38	738.41
Time 3 (s)	613.40	791.06	6846.50	12253.16
Max RAM	442.7 MiB	3.660 GiB	608.14 MiB	7.963 GiB
# Lines	4,266,280	37,497,133	5,867,324	81,963,950

Some Transmittance Results

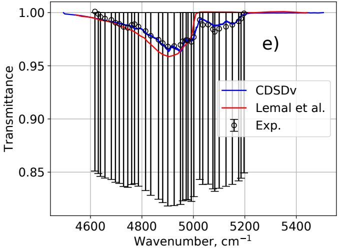

2.3 μm, $T = 1550$ K

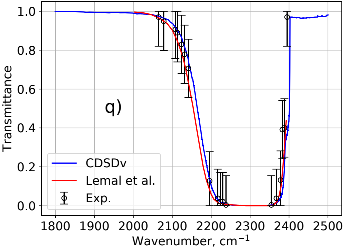

4.3 μm, $T = 1500$ K

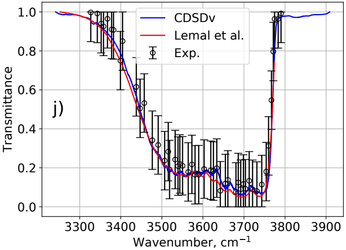

2.7 μm, $T = 1300$ K

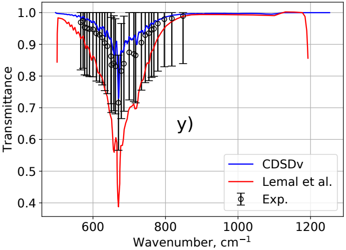

15 μm, $T = 2300$ K

Glow Discharge

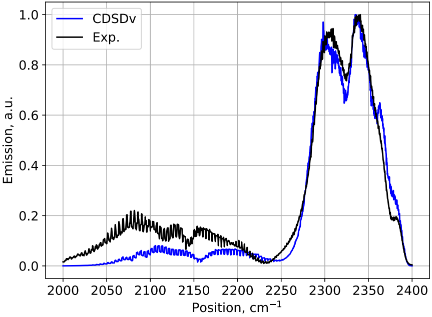

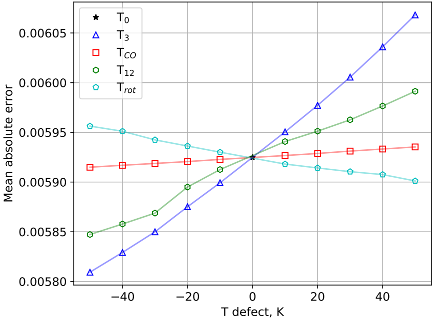

Einstein Coefficients

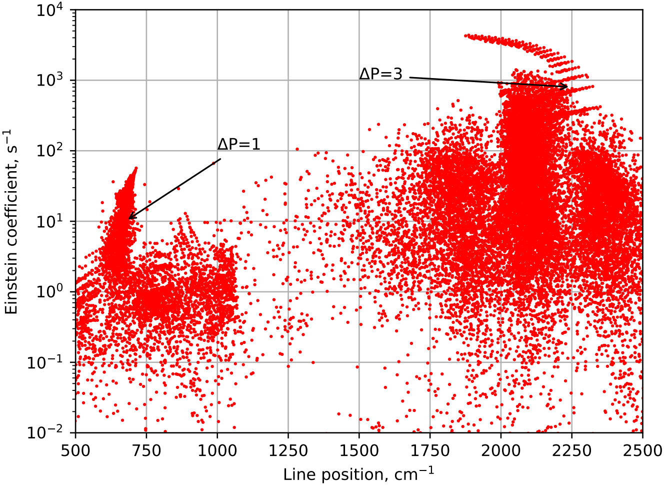

Polyads

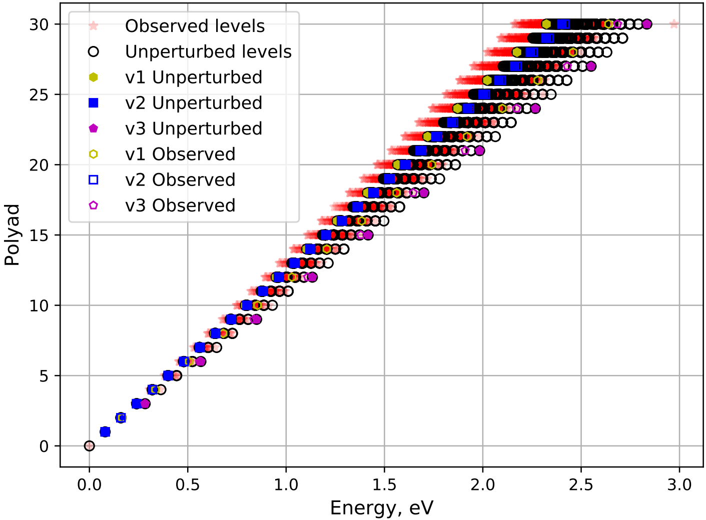

Observed levels
Unperturbed levels
v1 Unperturbed
v2 Unperturbed
v3 Unperturbed
v1 Observed
v2 Observed
v3 Observed
Polyad
Energy, eV
0
5
10
15
20
25
30
0.0
0.5
1.0
1.5
2.0
2.5
3.0

Prospective Shock-Tube Experiments

- Good experimental data still needed these days
- New experiments may bring more insight. A mix of time-dependent emission and absorption spectroscopy is very promising.
  - CO2 IR radiative emission
  - CO IR radiative emission
  - probing $O(^3P)$;$O(^1D)$ from the 130nm O transition. Is this possible?
  - probing O_2 from Schumann-Runge transition
- Dissociation and incubation times

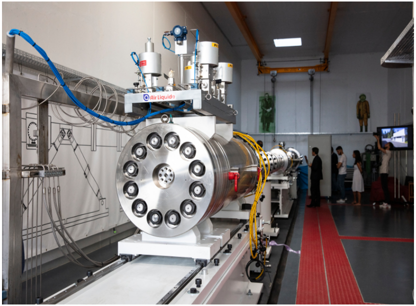

More Experiments

- Complementary to shock tubes, microwave plasmas and plasma torches can also contribute
- In addition to previous diagnostics:
  - CO_2 Chemiluminescence bands
  - Raman spectroscopy (?)
- Recombination experiments
- Relative high-T and steady state